

# Quantum correlations of two optical fields close to electromagnetically induced transparency

A. Sinatra

*Laboratoire Kastler Brossel, ENS, 24 Rue Lhomond, 75231 Paris Cedex 05, France*

We show that three-level atoms excited by two cavity modes in a  $\Lambda$  configuration close to electromagnetically induced transparency can produce strongly squeezed bright beams or correlated beams which can be used for quantum non demolition measurements. The input intensity is the experimental “knob” for tuning the system into a squeezer or a quantum non demolition device. The quantum correlations become ideal at a critical point characterized by the appearance of a switching behavior in the mean fields intensities. Our predictions, based on a realistic fully quantum 3-level model including cavity losses and spontaneous emission, allow direct comparison with future experiments.

PACS numbers: 42.50.Dv, 42.50.Gy, 42.65.Pc

Using optical nonlinearities it is possible to manipulate optical beams to the level of quantum fluctuations, producing squeezed states [1] that are important resources for quantum information with continuous variables [2]. Related to the field of squeezing is that of quantum non demolition (QND) measurements on an optical field, where quantum correlations between two different modes of the electromagnetic field are exploited to overcome the back-action noise of a quantum measurement [3]. Besides the fundamental interest in the theory of measurement, it was shown that QND correlations of propagating beams have direct application in quantum communication protocols as teleportation [4]. The best single back-action-evading measurement on optical beams was performed using cold atoms inside a doubly resonant cavity [5]. We suggest that these performances could be significantly improved by tuning the system close to the electromagnetically induced transparency (EIT) conditions [6].

Already in the nineties, theoretical studies showed that a lambda three-level medium close to EIT conditions in a cavity can be used to obtain squeezing [7]. Contrarily to previous proposals, here we assume that two different modes are resonant in the cavity. For small and symmetrical detunings from the upper level of  $\Lambda$  three-level atoms (see Fig.1), absorption is suppressed and the dispersive non linear response gives rise to a rich scenario where either self correlations (squeezing) or cross QND correlations can be established in the output beams. The correlations become ideal at a critical point that we characterize analytically. The technique we propose is experimentally accessible, and first experimental steps in this directions were done in atomic vapors without a cavity [8]. Here we show that the presence of the cavity is a crucial advantage especially if one can reach the good cavity limit.

We consider  $N$  atoms in a cavity excited by two modes symmetrically detuned from the upper level of a  $\Lambda$  three-level scheme as in Fig.1. For  $j = 1, 2$  let  $\omega_j$  be the frequency of field  $j$  and  $\hbar\omega_{aj}$  the energy of the corresponding

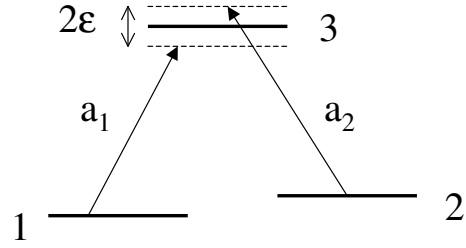


FIG. 1: Two cavity modes interact with the atoms in a  $\Lambda$  configuration close to EIT conditions.

atomic transition. We define  $\Delta_j = \frac{\omega_{aj} - \omega_j}{\gamma_w}$  the atomic detunings normalized to the decay rate of the optical coherences  $\gamma_w = (\gamma_1 + \gamma_2)/2$  where  $\gamma_1 + \gamma_2$  is the total population decay rate of the upper level;  $\theta_j = \frac{\omega_{cj} - \omega_j}{\kappa_j}$  the cavity detunings normalized to the cavity decay rates  $\kappa_j$ , and  $C_j = \frac{g_j^2 N}{\gamma_w \kappa_j}$  the cooperativities where  $g_j$  are the coupling constants for the two considered transitions. We use normalized variables proportional to the intracavity and input fields  $x_j = \frac{\sqrt{2}g_j}{\gamma_w} \langle a_j \rangle$  and  $y_j = \frac{\sqrt{2}g_j}{\gamma_w} \frac{2}{\sqrt{T_j}} E_j^{in}$  respectively, where  $T_j$  is the (input-output) mirror transmissivity for the field  $j$ . We name  $v$  and  $w$  the normalized polarizations between levels 1-3 and 2-3  $v = -(\sqrt{2}/N) \langle R^- \rangle$ ,  $w = -(\sqrt{2}/N) \langle S^- \rangle$  where  $R$  and  $S$  are collective operators constructed from the single atom operators  $|1\rangle\langle 3|$  and  $|2\rangle\langle 3|$  as in [9]. The master equation and the semiclassical equations describing the  $\Lambda$  system with two cavity fields, with the same notations introduced here, are given and discussed in detail in [10] where this model was successful to reproduce the experimental results of [5].

Let us consider a set of parameters symmetric for the two transitions:  $|y_j| = |y|$ ,  $C_j = C$ ,  $\gamma_j = \gamma$ ,  $\kappa_j = \kappa$ ,  $\theta_j = 0$  (empty cavity resonance for both fields), and let  $\Delta_1 = -\Delta_2 = \epsilon$  be small and positive. In Fig. 2 we show in rescaled units the stationary intensities of the intracavity fields  $I_j = |x_j|^2/4C\epsilon$  as a function of the common intensity of the input fields  $Y = |y|^2/4C\epsilon$ . With a solid

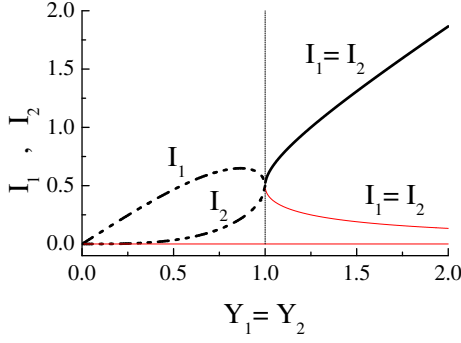


FIG. 2: Stationary intensities of the intracavity fields  $I_1$ , and  $I_2$  as a function of the common intensity of the input fields  $Y_1 = Y_2 = Y$ . In solid line the solution  $I_1 = I_2$ . The thick (red thin) line correspond to stable (unstable) solutions. In dashed-dotted line one of the two stable solutions with  $I_1 \neq I_2$ . Parameters:  $2\epsilon = 0.125$  and  $C_1 = C_2 = 250$ ,  $\gamma_1 = \gamma_2 = 10\kappa_1$ ,  $\kappa_2 = \kappa_1$ ,  $\theta_1 = \theta_2 = 0$ .

line we have plotted an  $S$ -shaped solution with  $I_1 = I_2$ . A stable branch of this solution appears for  $Y > 1$ . The negative slope branch and the lower branch very close to zero intensity are both unstable and play no role in the following. For  $Y < 1$ , apart from the solution  $I_1 = I_2$ , we get two other solutions with  $I_1 \neq I_2$ . In the figure we show one of them with  $I_1 > I_2$ . The second one is obtained by exchanging  $I_1$  and  $I_2$ . Both solutions are stable in the considered case  $\theta_1 = \theta_2 = 0$ .

We choose now two values of the input intensity, in turn above and below the turning point  $Y = 1$ , and show the stationary solutions for intracavity fields intensities as the cavity detunings vary in Fig. 3. The stable branches of these curves (thick lines) can be easily obtained experimentally by sweeping the cavity length [10]. We vary  $\theta_1$  and  $\theta_2$  keeping them always equal which would imply the use of two driving fields of close optical frequencies  $\Delta\lambda/\lambda \ll 1$  (and for example different polarizations). For  $Y = 1.05$  i.e. 5% above the turning point (upper half of Fig. 3) the stable solutions for the intracavity intensities are Lorentzian-looking curves symmetrically shifted by a small amount from their empty-cavity positions for both fields. Only for  $\theta_1 = \theta_2 = 0$  the two fields have the same stationary amplitude in the cavity corresponding to the stable high-transmission branch of the  $S$ -shaped curve in Fig. 2. For  $Y = 0.95$  i.e. 5% below the turning point (lower half of Fig. 3) the situation is rather different: the stable solution for the two fields *switches* between a high-intensity and a low-intensity curve being always  $I_1 \neq I_2$  although  $|y_1| = |y_2|$ . In contrast with the previous case this situation is very far from the independent-fields EIT solution and the fields are in fact strongly coupled.

Let us now introduce the useful correlations to characterize the quantum fluctuation properties of the system. For a given quadrature of the  $j^{th}$  field:  $X_j^\phi = a_j e^{-i\phi} +$

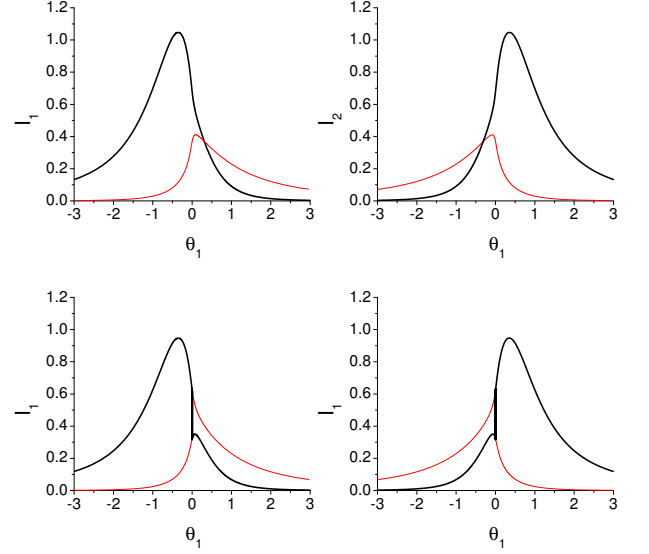


FIG. 3: Intracavity field intensities  $I_1$  (left half),  $I_2$  (right half) across the cavity scan. Upper half:  $Y = 1.05$ . Lower half:  $Y = 0.95$ . The thick (red thin) lines correspond to stable (unstable) solutions. The other parameters are as in Fig. 2.

$ia_j^\dagger e^{i\phi}$ , the squeezing spectrum is defined as

$$S_j^\phi(\omega) = 1 + 2\kappa_j \int_{-\infty}^{\infty} e^{-i\omega t} \langle : \delta X_j^\phi(t) \delta X_j^\phi(0) : \rangle dt \quad (1)$$

where  $\delta X_j^\phi$  denotes the time dependent fluctuation of the operator  $X_j^\phi$  around a steady state point. The column indicates normal and time ordering for the product inside the mean.  $S_j^\phi = 1$  is the shot noise and  $S_j^\phi = 0$  means total suppression of fluctuations in the quadrature  $X_j^\phi$ . The crossed correlations between the two fields are described by the coefficients  $C_s$ ,  $C_m$  and  $V_{s|m}$  [11] characterizing a QND measure of the amplitude quadrature  $X^{in}$  of one field, the *signal*, performing a direct measurement on the phase quadrature  $Y^{out}$  of the other field, the *meter*. Among the three coefficients  $C_s$  quantifies the non-destructive character of the measurement,  $C_m$  its accuracy and  $V_{s|m}$  refers to the “quantum state preparation” capabilities of the system.

$$C_s = C(X^{in}, X^{out}), \quad C_m = C(X^{in}, Y^{out}), \quad (2)$$

$$V_{s|m} = \langle X^{out}, X^{out} \rangle (1 - C(X^{out}, Y^{out})) \quad (3)$$

where for two operators  $A$  and  $B$  we define

$$C(A, B) = \frac{|\langle A, B \rangle|^2}{\langle A, A \rangle \langle B, B \rangle} \quad \text{with} \quad (4)$$

$$\langle A, B \rangle = \int_{-\infty}^{+\infty} e^{-i\omega t} \frac{1}{2} \langle A(t)B + BA(t) \rangle dt. \quad (5)$$

Superscripts *in* and *out* refer to the input and output cavity fields. By calling  $\phi_j^{in}$  and  $\phi_j^{out}$  the phases of the

input and output fields in steady state, and choosing field 1 as the *meter* and field 2 as the *signal*, we define  $X^{out(in)} = X_2^{\phi^{out(in)}}$  and  $Y^{out} = Y_1^{\phi^{out} + \pi/2}$ . For an ideal QND measurement  $C_m = C_s = 1$ , and  $V_{s|m} = 0$ .

The quantum fluctuations counterpart of Fig. 3 (top) is shown in Fig. 4 (top) where squeezing of the output fields optimized with respect to the quadrature  $S_j^{best}(\omega = 0)$  is plotted as a function of the cavity detuning. A large amount of squeezing is present in both fields close to  $\theta_1 = 0$ . As one can see from Fig. 3 (top) the two fields are well transmitted by the cavity for  $\theta_1 = 0$ , and the system efficiently converts the input coherent beams into bright squeezed beams. Correspondingly to Fig. 3 (bottom) for  $Y = 0.95$ , in Fig. 4 (bottom) we plot the coefficients  $C_s$ ,  $C_m$  and  $V_{s|m}$  across the cavity scan. The useful quantum correlations are calculated by a linearized treatment of quantum fluctuations around the stable stationary solution as in [10]. Despite the fact that the two fields have different intracavity intensities at  $\theta_1 = 0$ , they play here symmetrical roles for the QND scheme; the figure corresponding to the reversed scheme  $1 \leftrightarrow 2$  being obtained by reflection of the plots  $\theta_1 \leftrightarrow -\theta_1$ .

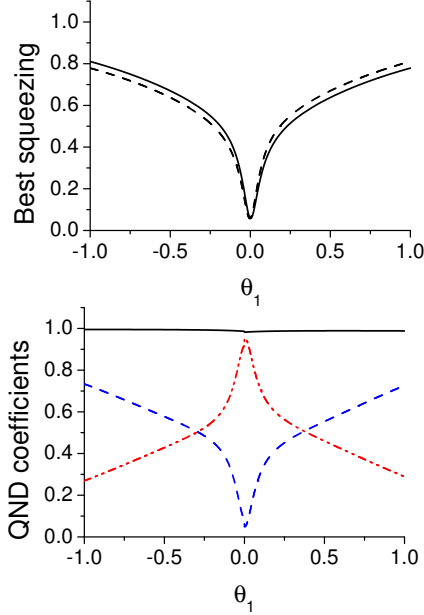


FIG. 4: Top: Best squeezing of the fields across the cavity scan for  $Y = 1.05$  and  $\omega = 0$ . Squeezing of field 1 (2) is plotted with a solid (dashed) line. Bottom: QND coefficients across the cavity scan for  $Y = 0.95$  and  $\omega = 0$ .  $C_m$  (red dashed-dotted line),  $C_s$  (solid line),  $V_{s|m}$  (blue dashed line). Parameters as in Fig.3.

We show in Fig. 5 the frequency dependence of the quantum correlations both below and above the turning point  $Y = 1$ , for a fixed value of the cavity detuning close to zero. For values of the cooperativity parameters currently obtained in experiments, QND coefficients such as  $C_s = 0.98$ ,  $C_m = 0.95$ ,  $V_{s|m} = 0.05$  can be achieved

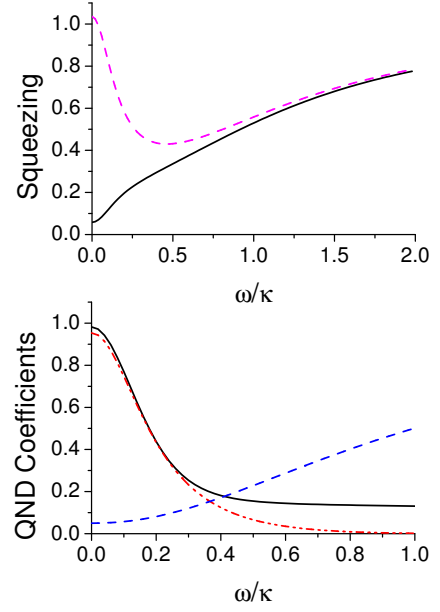


FIG. 5: Top: Squeezing spectra of field 1, for  $Y = 1.05$  in the center of the cavity scan ( $\theta_1 = 0.0013$ ). Best squeezing in solid line and amplitude squeezing  $S_1^{\phi^{out}}$  in purple dashed line. Bottom: QND spectra for  $Y = 0.95$  and  $\theta_1 = 0.0018$ .  $C_m$  (red dashed-dotted line),  $C_s$  (solid line),  $V_{s|m}$  (blue dashed line). The other parameters are as in Fig.2.

in this regime, representing a significant improvement with respect to previously obtained results [5] based on the so called “ghost transition” scheme [12], [10]. Although we concentrate here on the good cavity limit, in which as we will show the quantum correlations become ideal approaching the turning point  $Y = 1$ , some QND correlations between the two modes persist also in the bad cavity limit. For example for  $\epsilon = 0.25$ ,  $C = 25$ ,  $\kappa = 3\gamma$ ,  $\theta_1 = 6 \times 10^{-3}$ ,  $Y = 0.9$  and  $\omega = 0.1\gamma$  we get  $C_s = C_m = 0.72$ ,  $V_{s|m} = 0.26$ .

In the limit of weak atomic detunings, useful analytical results can be obtained. The analytical solution of the semiclassical equations of the system at steady state is given in [10]. By expanding the steady state polarizations  $v$  and  $w$  to the first order in  $\epsilon$  we obtain

$$v = i \frac{4\epsilon x_1 |x_2|^2}{(|x_1|^2 + |x_2|^2)^2} \quad w = -i \frac{4\epsilon x_2 |x_1|^2}{(|x_1|^2 + |x_2|^2)^2}. \quad (6)$$

By inserting (6) in the equations for the intracavity fields amplitudes, with  $|y_j| = |y|$ ,  $\theta_j = 0$  and  $C_j = C$ , we obtain at steady state a “universal solution” for rescaled field intensities. For  $Y < 1$  there are two stable solutions

$$I_1 = \frac{Y}{2} (1 \pm \eta); \quad I_2 = \frac{Y}{2} (1 \mp \eta) \quad (7)$$

where  $\eta = \sqrt{1 - Y^2}$ . For  $Y > 1$ , out of two solutions

$$I_1 = I_2 = I; \quad I = \frac{Y}{2} \left( 1 \pm \sqrt{1 - \frac{1}{Y^2}} \right) \quad (8)$$

the one with the plus sign is stable and the other one unstable. Solutions (7)-(8) are indistinguishable from those of the full three-level model in Fig. 2. The phases of the input fields with respect to intracavity fields (which are taken real at steady state) are  $\phi_1^{in} = \text{atan}[\sqrt{I_2/I_1}]$ ,  $\phi_2^{in} = -\text{atan}[\sqrt{I_1/I_2}]$  for  $Y < 1$ , and  $\phi_1^{in} = \text{atan}[1/2I] = -\phi_2^{in}$  for  $Y > 1$ . For the output fields  $\phi_1^{out} = -\phi_1^{in}$ ,  $\phi_2^{out} = -\phi_2^{in}$  in both cases.

In order to study the quantum properties of the system analytically we further assume that (i)  $\gamma \gg \kappa$  so that the atomic fluctuations follow adiabatically the field fluctuations, and (ii) the noise from spontaneous emission is negligible, which we found true when the cooperativity is large enough. In this limit, using the steady state polarizations (6), we can solve analytically the equations for the field fluctuations and obtain the correlation functions.

For  $Y > 1$  and  $I_1 = I_2 = I$  and taking  $\kappa^{-1}$  as the unit of time, we obtain

$$\delta \dot{x}_j = -\delta x_j + i \frac{(-1)^{3-j}}{2I} \delta x_j^* \quad j = 1, 2. \quad (9)$$

These equations describe two independent two-photon processes for which instabilities and squeezing have been studied extensively [13]. The best squeezing spectrum for each field is

$$S_j^{best}(\omega) = 1 - \frac{4a}{(1+a)^2 + \omega/\kappa^2}, \quad a = \frac{1}{2I}, \quad (10)$$

yielding perfect squeezing at zero frequency at the turning point where  $Y = 1$ ,  $I = 0.5$  and  $a = 1$ .

For  $Y < 1$  and  $I_1 \neq I_2$  the fluctuations of the two fields are coupled. For  $I_1 > I_2$  we get

$$\delta X_1 = -\delta X_1 - i \frac{1-\eta}{Y} \delta Y_1 \quad (11)$$

$$\delta Y_1 = -\delta Y_1 + i \frac{1+\eta}{Y} \delta X_1 - 2i \eta \delta X_2. \quad (12)$$

The equations for field 2 are obtained from (11) and (12) by changing the sign in front of  $\eta$  and of  $i$ . Simple analytical expressions can be obtained for the squeezing and the conditional variance  $V_{s|m}$  of the fields at  $\omega = 0$

$$S_j^{int} = S_j^{best} = 1; \quad S_j^{phase} = -3 + \frac{4}{\eta^2} \quad (13)$$

$$V_{s|m} = \frac{\eta^2}{4 - 3\eta^2} \quad (14)$$

showing that the fields have diverging phase noise and become perfectly correlated at the turning point. We checked that the spectra in Fig. 5 are well reproduced by the analytical results.

In conclusion, in a symmetrically detuned EIT scheme, and for equal input intensities  $Y$  of the two fields we have shown the existence of a universal  $S$ -shaped steady state

curve (Fig.2) which divides the parameter space into two parts: for input intensities higher than the upper turning point of the curve, the quantum fluctuations of the fields become quadrature dependent and can be reduced in a quadrature, while for input intensities lower than the turning point, crossed phase-intensity quantum correlations build up between the two fields. The system becomes a perfect “squeezer” or an ideal QND device at the turning point. The “universal” point  $Y = 1$ , can be identified experimentally by the appearance of the switching behavior described in Fig.3, and can be used as a reference in the parameter space to choose either the squeezing or the QND effect and to optimize it. An implementation using either a vapor [8], or a trapped cold atoms in an optical cavity [5],[14],[15] seems within the reach of present technology.

I thank L. Lugiato and P. Grangier for useful discussions, M. Guerzoni for her contribution to this work and Y. Castin for comments on the manuscript. LKB is UMR 8552 du CNRS de l'ENS et de l'UPMC; support from IFRAF is acknowledged.

- 
- [1] For a recent review on squeezing see e.g. H. Bachor, “A Guide to Experiments in Quantum Optics”, Wiley-VCH (2004).
  - [2] S.L. Braunstein, P. van Loock, Rev. of Mod. Phys. **77**, 513 (2005).
  - [3] P. Grangier, A. Levenson, J.-Ph. Poizat, Nature **396**, 537 (1998).
  - [4] D. B.Horoshko, S.Ya. Kilin, Phys. Rev. A **61**, 032304 (2000).
  - [5] J-F. Roch, K. Vigneron, P. Grelu, A. Sinatra, J-P. Poizat, P. Grangier, Phys. Rev. Lett. **78**, 634 (1997).
  - [6] For a review on EIT see e.g. M. Fleischhauer, A. Imamoglu, J.P. Marangos, Rev. Mod. Phys. **77**, 633 (2005);
  - [7] K.M. Gheri, D.F. Walls, M.A. Marte, Phys. Rev. A **50**, 1871 (1994).
  - [8] V.A. Sautenkov, Y.V. Rostovstev, M.O. Scully, Phys. Rev. A **72**, 065801 (2005), C.L. Garrido Alzar, L.S. Cruz, J.G. Aguirre Gómez, Europhys. Lett. **61**, 485 (2003).
  - [9] L.A.Lugiato *Progress in Optics XXI*, edited by E. Wolf (North-Holland, Amsterdam, 1977), p. 71.
  - [10] A. Sinatra, J-F. Roch, K. Vigneron, P. Grelu, J-P. Poizat, K. Wang, P. Grangier, Phys. Rev. A **57**, 2980 (1998).
  - [11] M. Holland, M. Collett, D.F. Walls, M.D. Levenson, Phys. Rev. A **42**, 2995 (1990); J.Ph. Poizat, J.-F. Roch and P. Grangier, Ann. Phys. (Paris) **19**, 265 (1994).
  - [12] K.M. Gheri, P. Grangier, J.-Ph. Poizat, D. Walls, Phys. Rev. A **46**, 4276 (1992).
  - [13] L. Lugiato, P. Galatola, L. Narducci, Opt. Comm. **76**, 276 (1990).
  - [14] V. Josse, A. Dantan, A. Bramati, M. Pinard, E. Giacobino, Phys. Rev. Lett. **92**, 123601 (2004);
  - [15] J.K. Thompson, J. Simon, H. Loh, V. Vuletić, Science **313**, 74 (2006).